Monte Carlo and Molecular Dynamics Simulation of the Glass Transition of Polymers

Kurt Binder, Jörg Baschnagel, Christoph Bennemann and Wolfgang Paul
Institut für Physik, Johannes-Gutenberg-Universität, Mainz D-55099 Mainz, Staudinger Weg 7, Germany

Abstract

Two coarse-grained models for polymer chains in dense glass-forming polymer melts are studied by computer simulation: the bond fluctuation model on a simple cubic lattice where a bond-length potential favors long bonds is treated by dynamic Monte Carlo methods, and a bead-spring model in the continuum with a Lennard-Jones potential between the beads is treated by Molecular Dynamics. While the dynamics of both models differ for short length scales and associated time scales, on mesoscopic spatial and temporal scales both models behave similarly. In particular, the mode coupling theory of the glass transition can be used to interpret the slowing down of the undercooled polymer melt. For the off-lattice model, the approach to the critical point of mode coupling is both studied for constant pressure and for constant volume. The lattice model allows a test of the Gibbs-Di Marzio entropy theory of the glass transition, and our finding is that although the entropy does decrease significantly, there is no "entropy catastrophe" where the fluid entropy would turn negative. Finally, an outlook on confinement effects on the glass transition in thin film geometry is given.

Contribution to the II Workshop on Non Equilibrium Phenomena in Supercooled Fluids, Glasses and Amorphous Materials, Pisa 1998, submitted to *J. Phys.: Condens. Matter* on Sept. 27, 1998

I. INTRODUCTION

The glass transition from the supercooled melt to the amorphous solid still is a puzzle [1–4]. While the viscosity $\eta(T)$ increases about 15 orders of magnitude (T_g is empirically defined by $\eta(T = T_g) = 10^{13}$ Poise) in a narrow temperature interval, the change in the static structure factor $S(q)$ (q is the scattering wavenumber) is rather minor, see e.g. [5]. What is then the physical basis that many different systems show a nearly universal phenomenology of relaxation {e. g., increase of relaxation time τ or $\eta(T)$ [$\eta(T) \propto \tau$] described by the Vogel-Fulcher-Tammann (VFT) law, $\ln\tau \propto \ln\eta \propto E_{\rm VF}/(T - T_{\rm VF})$ [1], relaxation functions obey the Kohlrausch-Williams-Watts (KWW) law, $\varphi(t) \propto \exp\left[-(t/\tau)^{\beta}\right]$, etc. [1]}?

The answer to this question is controversial: e.g., there is the idea of an "entropy catastrophe" static phase transition underlying the glass transition {the configurational entropy

of the undercooled fluid vanishes at $T_0 < T_g$ [6], with possibly [7] $T_0 = T_{\rm VF}\}$. Mode coupling theory [2], on the other hand, yields a (rounded [8]) dynamical transition from an ergodic fluid (atoms easily can escape from the cages formed by their neighbors) at a “critical” temperature $T_c > T_g$ to a nonergodic state (“structural arrest”). Still other concepts attribute the increase of τ upon cooling to the increase of a glass correlation length [9], in analogy with spin glasses [10].

Polymer melts can be held in very good metastable equilibrium in their supercooled state, and their T_g's occur in an experimentally convenient range, and thus a wealth of experimental data exists. Thus it is desirable to approach these systems also by theoretical modeling via computer simulation [11]. However, due to the large size of these polymer coils (they exhibit nontrivial structure from the Å scale of covalent bonds up to the gyration radius which can be 100 Å) and the many decades of time scales spanned by the relaxation times of their motion simulation of polymers is very difficult, and requires to use simplified efficient models [11]. Two such models will be defined and compared in the next section, while Sec. 3 describes the tests of mode coupling theory performed with these models. Sec. 4 briefly describes tests of other theories and contains also some concluding remarks.

II. COARSE-GRAINED MODELS FOR POLYMERS ON THE LATTICE AND IN THE CONTINUUM

The basic idea is to eliminate both the structural details on very small scales and the associated very fast dynamics by using a coarse-graining along the chemical sequence of the chains [11]: $n \approx 3 - 5$ successive chemical units are mapped into one effective bond, connecting two effective monomers. These effective bonds may be defined on a lattice as well as in the continuum. In the lattice case, the effective monomers are formed from all 8 sites of an elementary cube on the lattice, and no site may belong to more than one monomer (excluded volume interaction). Bond lengths in this “bond fluctuation model” [11] are taken in the range from 2 to $\sqrt{10}$ lattice spacings, and bond vectors $\vec{b} = (\pm 3, 0, 0)$ [or permutations thereof] are taken to be in the ground state, while all other choices of the bond vector represent excited states, which an energy cost $\varepsilon(= 1$; also $\mathrm{k_B} \equiv 1)$. This bond length potential may be thought of as representing the original atomistic intrachain potentials in a coarse-grained way. Since this particular choice of the potential has the effect that each bond that is in the ground state blocks the 4 sites between its adjoining effective monomers from further occupation, it has the effect that free volume in the dense system is “wasted” and a “geometric frustration” is created - at high densities not enough free volume is available that all bonds manage to get into their ground state as $T \to 0$ [12]. This model can be simulated very efficiently, and for chain lengths N as small as $N = 10$ properties typical of polymers (e g. gyration radius $\left\langle R_g^2 \right\rangle^{1/2} \propto \sqrt{N}$) are reproduced. A density of $\phi = 0.533$ of occupied sites corresponds to a dense melt [12,13].

Dynamics is introduced by randomly selecting a monomer of a chain and by attempting to move it by one lattice unit in a randomly chosen direction. Of course, the move is only carried out if the new position satisfies excluded volume and bond length constraints, and the possible energy change is considered with the usual Metropolis criterion [11,12]. It is thought that this “random hopping” of effective monomers in a coarse-grained sense corresponds to

the random hops of chemical bonds over barriers in the torsional potential, because by such moves pieces of a chain can rotate relative to each other, and thus are responsible for the relaxation of chain configurations [11,14]. If one carries out such a mapping of a realistic (i.e., atomistic) chain model on the bond fluctuation model literally, one estimates that one attempted Monte Carlo step (MCS) per monomer corresponds to 10^{-13} sec, and the lattice unit to a distance of 2Å [14]. Typically, runs are carried out for systems of $L \times L \times L$ with periodic boundary conditions and $L = 30$, averaging over 16-160 independent "replicas" of the system over a time of up to 10^7 MCS. Thus even for the time window of this coarse-grained model we are restricted to $t \approx 1\mu$sec (while molecular dynamics simulations of atomistic models can deal with $t<1$nsec only). However, one important aspect is that one can equilibrate the system configurations also with artificial moves, which have no counterpart in the dynamics of real chains, such as the "slithering snake" algorithm [11,14], and thus gain several orders of magnitude in time due to faster relaxation. In this way, configurations of the well equilibrated melts are prepared at rather low temperatures, which serve as initial states for runs with the "random hopping" algorithm studying the dynamics of these melts.

Alternatively, we treat a continuum model where an effective bond is represented by a (finitely extensible) spring, and the effective monomers are the beads of this bead-spring model. There is a Lennard-Jones interaction between any pair of beads cut off at a distance $r_c = 2 \times 2^{1/6}\sigma$ [15],

$$U_{\mathrm{LJ}}(r) = 4\varepsilon\left[(\sigma/r)^{12} - (\sigma/r)^6\right] + c, \tag{1}$$

the constant c being chosen such that $\mathrm{U}_{\mathrm{LJ}}(r_c) = 0$. Choosing here units of length and temperature such that $\sigma = 1$, $\varepsilon = 1$, the springs are described by

$$U(r) = -\frac{1}{2}kR_0^2 \ln\left[1 - (r/R_0)^2\right], \qquad R_0 = 1.5, \quad k = 30. \tag{2}$$

While $\mathrm{U}_{\mathrm{LJ}}(r)$ has its preferred distance at a minimum for $r_{\min} = 2^{1/6}$, the minimum of the potential between neighboring monomers along the chain (given by the sum of Eqs. (1), (2)) occurs for $r_0 \approx 0.96$: although the bead-spring model is fully flexible, this incompatibility of $r_0/r_{\min}$ with any standard crystal structure prevents crystallization of our model, and thus creates the "frustration" in the fluid necessary for the formation of a glass upon cooling.

This off-lattice model is simulated by NpT-molecular-dynamics, choosing also a chain length of $N = 10$, and altogether $M = 1200$ monomers in the system [15]. Note that the constant pressure ensemble [16] is used for equilibration only - for a study of dynamic properties a clock is set to zero and runs are started at $T =$const (using a suitable Nosé-Hoover thermostat [17]) which produce a dynamical behavior practically indistinguishable from the microcanonical ensemble [15].

Fig. 1 shows that one obtains the structure factor $S(q)$ of the amorphous polymer melt in close similarity with the experiment [5]. If one studies the volume $v(T)$ per effective monomer in a slow cooling run, starting at $p = 1$ from a well-equilibrated configuration at $T = 0.6$ and lowering T every 500 000 MD time steps by 0.02, one finds a rather well-defined kink at $T_g \approx 0.41$, while a fit of the self-diffusion constant to the Vogel–Fulcher law yields $T_{\mathrm{VF}} \approx 0.33$ [18]. Thus the model does exhibit a glass transition, as expected.

The bond fluctuation model also yields $S(q) \approx 0$ for small q due to the very small compressibility of the polymer melt, and then a broad peak similar to the "amorphous

halo" of Fig. 1 occurs, at $q \approx 3$ (in units of the lattice spacing for this model; physically this corresponds to about 1.5 Å^{-1}) [13]. The peak position and shape also change very little with temperature. However, the second shallow and temperature-independent peak of Fig. 1 at still larger q, representing intra-chain correlations, is less well reproduced [13]. This is not surprising, since $q = 2\pi$ corresponds in real space to one lattice unit. A further disadvantage of the lattice model is that one can study the glass transition only at constant volume, while in the off-lattice model both constant volume and constant pressure studies were performed [18].

III. TESTING THE MODE COUPLING THEORY (MCT) OF THE GLASS TRANSITION

Fig. 2 shows the intermediate incoherent dynamic structure factor $F_q(t)$, defined as

$$F_q(t) = \frac{1}{M} \sum_{i=1}^{M} \langle \exp\{i\vec{q} \cdot [\vec{r}_i(t) - \vec{r}_i(0)]\} \rangle \,, \tag{3}$$

where the sum is over all M monomers in the system (which are at position $\vec{r}_i(t)$ at time t). Pronounced two-step relaxation is seen, the second step ("α-relaxation") satisfies the time-temperature-superposition principle, while the first step ("beta relaxation") does not [15]. The relaxation time τ_q is both compatible with the Vogel-Fulcher law with $T_{\mathrm{VF}} \approx 0.33$, and with a power law (Fig. 3) but with a q-dependent exponent γ_q [18]. While the consistency with a power law is evidence in favor of MCT [2], the q-dependence of the exponent γ_q is not. In addition, one sees that the data deviate from the power law both for $T/T_c - 1 \gtrsim 0.4$ (as expected, since one has left the asymptotic region) and for $T/T_c - 1 \lesssim 0.04$ (which can be attributed to "hopping processes" by which effective monomers can escape from the cage formed by their neighbors, and requires use of the extended version of the theory [8] that describes the rounding of the ergodic to nonergodic transition). Thus, the observability of the idealized MCT [2] is restricted to about one decade in $T/T_c - 1$, showing the limitations of this theory when applied to polymers [15,18,19].

In the α-regime $F_q(t)$ can be fitted to the KWW law with an exponent β that is also weakly q-dependent ($\beta_q = 0.70 \pm 0.08$ for $q = 6.9$ [15]); for a detailed analysis of this q-dependence see Ref. [19]). The predictions of MCT for the β regime can also be tested in detail and compare rather favorably with MCT [19], although the same caveat over the restricted "temperature window" where MCT is applicable must again be made.

This analysis can be replaced for several pressures and thus one can trace out a "critical line" $T_c(p)$ in the (T, p) plane separating the liquid from the ideal glass (Fig. 4). Carrying out simulations at constant pressure and at constant density that lead to the same point $(T_c(p), p)$ on the line, one finds that indeed $\tau_q \propto (T - T_c)^{-\gamma_q}$ holds with the same T_c and the same γ_q for both paths in the (T, p) plane. This underscores that the MCT critical line is indeed physically significant.

Also the bond fluctuation model has been compared to MCT, both in its idealized [20] and extended [21] version. While a fit of various relaxation times and of the selfdiffusion constant to the VF law is nicely compatible with the data and yields $T_{\mathrm{VF}} \approx 0.125 \pm 0.005$ [22], the MCT fits both [20,21] yield $T_c \approx 0.15$, and power law behavior occurs over a similar

temperature interval as for the continuum model. One characteristic difference between both models concerns the β-relaxation regime, however: while in the off-lattice model the first decay of the structure factor $F_q(t)$ {Fig. 2} is due to small-amplitude motions (over distances of the order of 10% of the distances between effective monomers and their nearest neighbors), no such small scale motion is possible in the bond fluctuation model: either a monomer hops a lattice unit), or it cannot hop at all. This distinction also shows up when we compare the time dependence of the scaled mean square displacements of monomers for both models (Fig. 5). Both the lattice model and the continuum model are thought to correspond essentially to the same physical system, a dense melt of short polymers, on a coarse-grained level. This implies that on mesoscopic scales (length scales of the order of the distance between effective monomers or larger) these different coarse-grained models should yield very similar results. Comparing suitably scaled data, so that units of length and time are absorbed in the scales, this is indeed the case (Fig. 3). Note that the regime where MCT is applicable is actually the regime of rather small displacements, up to the order of distances between monomers,from where on then a Rouse-like behavior controls the dynamics.

IV. COMMENTS ON OTHER THEORETICAL CONCEPTS AND SOME CONCLUDING REMARKS

A particular advantage of the lattice model is that the slithering snake algorithm allows to obtain equilibrium properties of the model at fairly low temperatures, and also the configurational entropy $S(T)$ can be computed [23] in order to test the Gibbs-Di Marzio theory [6]. Indeed one finds that $S(T)$ decreases to about 1/3 of its high temperature value $S(\infty)$ as T approaches T_g, but there the curve $S(T)$ vs T bends over and gives evidence that $S(T)$ stays nonzero at lower temperatures. Conversely, if one extracts the quantities that are used in the theory [6] directly from the simulation and inserts them into the (approximate!) theoretical formula [6,23], one would find an "entropy catastrophe" $\{S(T)$ becoming negative$\}$ at $T \lesssim 0.18$. This unphysical result, however, is easily traced back to a severe underestimation of $S(\infty)$ by the approximations of [6]. The "entropy catastrophe" [6] thus clearly is an artefact of an inaccurate approximation, one should not attribute physical significance to it. In such manner simulations can go beyond experiment for testing theories, because the input parameters of the theories can be unambiguously extracted from the simulation as well, and a comparison between theory and simulation is possible without adjustable parameters whatsoever.

It is interesting to note that nevertheless the Adam-Gibbs equation [7], $D/D_0 \propto \exp\{-E_{\mathrm{act}}/TS(T)\}$, where D_0 is the self-diffusion constant at very high temperatures and E_{act} some activation energy, provides a very good description of the diffusion constants found in the simulation when one uses also the $S(T)$ found in the simulation (Fig. 6). At the same time, the absence of any finite size effect in Fig. 6 is at odds with the idea to attribute the slowing down implied by the decrease of $D(T)$ to an increasing glass correlation length $\xi(T)$ [9], via $\tau(T) \propto [\xi(T)]^z$ with z a dynamic exponent [10]: if such an hypothesis would hold, one would expect that decreasing L should decrease $\xi(T)$ [since $\xi(T) \leq L$] and hence $\tau(T)$, and in turn $D(T)$ should increase with increasing L. Fig 6 proves the absence of such finite size effects. This finding is surprising, since a growing static length can be extracted both from

the pair correlation function in the melt [24] and from surface effects near hard walls [25]. It hence appears that there is a growing length identified in [24,25] but it is not responsible for the slowing down at T_g. Of course, there is no contradiction with experimental results which find that T_g in thin films (or in pores, respectively) changes when the linear dimension of the film (or pore respectively) is varied: depending on the boundary conditions at the surface, the local mobility of monomers in the surface region changes, and this effect is the more pronounced on the freezing the smaller the linear dimension. No such surface effect is present with the periodic boundary conditions in Fig. 6, of course. In experiments on the glass transition in confined systems, finite size effects and surface effects can never be clearly separated, unlike simulations where one can show that there is no finite size effect (Fig. 6) at least in the temperature region studied here, although there do exist surface effects [25].

Returning to MCT, we emphasize that idealized MCT does provide a good description of a large number of simulation data, but only over a rather restricted range of temperatures (about one decade in $T/T_c - 1$) and corresponding times (or viscosities, typically the range $10^0 < \eta(T) < 10^2$ Poise if $\eta(T_c) = 10^3$ Poise: the huge range from $10^3 \leq \eta \leq 10^{13}$ Poise is outside the scope of the theory). Correspondingly, only a small intermediate regime of small monomer displacements in Fig. 5 is described - neither the initial increase that depends on microscopic properties of the model, nor the regime of hopping processes that lead to a Rouse-like relaxation of coil configurations (before ultimately ordinary diffusion sets in) are part of the theory. Since there occur smooth crossovers between the various regimes, a reliable assessment of the validity of MCT for polymer melts near T_g is difficult. A more complete theory (that unifies e.g. MCT and the Rouse model) would be very desirable.

Acknowledgements: We are grateful to S. Böhmer, K. Okun, V. Tries and M. Wolfgardt, who have contributed to earlier stages of this work, for their fruitful collaboration. We acknowledge the financial support from the Deutsche Forschungsgemeinschaft (DFG), grant No SFB262/D2, and we thank the Höchstleistungsrechenzentrum Jülich (HLRZ) and the Regionales Hochschulrechenzentrum Kaiserslautern (RHRK) for generous grants of computer time.

REFERENCES

[1] J. Jäckle, Rep. Progr. Phys. **49** (1986) 171.

[2] W. Götze and J. Sjögren, Rep. Progr. Phys. **55** (1992) 241.

[3] J. Zarzycki (ed.) *Materials Science and Technology, Vol. 9: Structure and Properties of Glasses* (VCH, Weinheim 1991).

[4] K. L. Ngai (ed.) *Proc. 3rd Intl. Discussion Meeting on Relaxations in Complex Systems* [J. Noncryst. Solids **235–237** (1998)].

[5] D. Richter, B. Frick and B. Farago, Phys. Rev. Lett. **61** (1988) 2465; A. Arbe, U. Buchenau, L. Willner, D. Richter, B. Farago and J. Colmenero, Phys. Rev. Lett. **76** (1996) 1872.

[6] J. H. Gibbs and E. A. Di Marzio, J. Chem. Phys. **28** (1958) 373, 807.

[7] G. Adam and J. H. Gibbs, J. Chem. Phys. **43** (1965) 139.

[8] M. Fuchs, W. Götze, S. Hildebrand and A. Latz, J. Phys.: Condens. Matter **4** (1992) 7709.

[9] E. Donth, *Relaxation and Thermodynamics of Polymers: Glass Transition* (Akademie-Verlag, Berlin 1992).

[10] K. Binder and A. P. Young, Rev. Mod. Phys. **58** (1986) 801.

[11] K. Binder (ed.) *Monte Carlo and Molecular Dynamics Simulations in Polymer Science* (Oxford University Press, New York 1995).

[12] J. Baschnagel, K. Binder and H. P. Wittmann, J. Phys.: Condens. Matter **5** (1993) 1597.

[13] J. Baschnagel and K. Binder, Physica A **204** (1994) 47.

[14] V. Tries, W. Paul, J. Baschnagel and K. Binder, J. Chem. Phys. **106** (1997) 738.

[15] C. Bennemann, W. Paul, D. Binder, and B. Dünweg, Phys. Rev. E **57** (1998) 843.

[16] W. G. Hoover, Phys. Rev. A 34 (1986) 2499.

[17] S. Nosé, Progr. Theor. Phys. Suppl. **103** (1991) 1; W. G. Hoover, Phys. Rev. A **31** (1985) 1695.

[18] C. Bennemann, W. Paul, J. Baschnagel, and K. Binder *Investigating the influence of different thermodynamic paths on the structural relaxation via glass forming polymer melt*, submitted to J. Phys.: Condens. Matter.

[19] C. Bennemann, J. Baschnagel and W. Paul, *Molecular Dynamics simulation of a glassy polymer melt: incoherent scattering function*, submitted to Phys. Rev. E, cond-mat/9809335.

[20] J. Baschnagel, Phys. Rev. B **49** (1994) 135.

[21] J. Baschnagel and M. Fuchs, J. Phys.: Condens. Matter **7** (1995) 6761.

[22] K. Okun, M. Wolfgardt, J. Baschnagel and K. Binder, Macromolecules **30** (1997) 3075.

[23] M. Wolfgardt, J. Baschnagel, W. Paul and K. Binder, Phys. Rev. E **54** (1996) 1535.

[24] K. Binder, J. Baschnagel, S. Böhmer and W. Paul, Phil. Mag. B **77** (1998) 591.

[25] J. Baschnagel and K. Binder, Macromolecules **28** (1995) 6808.

FIGURES

FIG. 1. Structure factor $S(q)$ plotted vs wavenumber q, for a system of 120 off-lattice bead-spring chains with chain length $N = 10$, simulated in the NpT-ensemble at scaled pressure $p = 1$, choosing Lennard-Jones units $\varepsilon = 1, \sigma = 1$ (and $k_{\rm B}$=1). Note that the zero of the ordinate for each curve is shifted upward by 0.001 relative to the previous one. From Bennemann et al. [15].

FIG. 2. Dynamic structure factor $F_q(t)$ of the off-lattice model at scaled pressure $p = 1$ plotted vs a rescaled time t/τ_q (where τ_q is defined from $F_q(t = \tau_q) = 0.3$) for $q = 6.9$, the peak position of the static structure factor at low T (cf. Fig. 1). Only temperatures in the range $0.46 \leq T \leq 0.7$ are included, as indicated. From Bennemann et al. [15].

FIG. 3. Log-log plot of the relaxation time τ_q versus $T - T_c$ with $T_c = 0.45$, for a pressure $p = 1$ and three values of q. The straight lines indicate the power laws $\tau_q \propto (T - T_c)^{-\gamma_q}$ with exponents $\gamma_q = 2.3$, 2.1 and 2.0 (from above to below). From Bennemann et al. [18].

FIG. 4. Critical line $T_c(p)$ in the (T, p) plane, for the off-lattice bead spring model. From Bennemann et al. [18].

FIG. 5. Comparison of the mean-square displacement $g_1(t)$ of inner monomers $\{g_1(t) \equiv \left\langle [\vec{r}_i(t) - \vec{r}_i(0)]^2 \right\rangle\}$ plotted vs scaled time $\{Dt/\langle R_g^2\rangle$, D being the selfidiffusion constant and $\langle R_g^2\rangle$ the mean square gyration radius of the chains$\}$ for the off-lattice model (curve marked MD) with the corresponding Monte Carlo results for the bond fluctuation model at three temperatures.

FIG. 6. Selfdiffusion constant of the bond fluctuation model plotted vs inverse temperature, for $L \times L \times L$ lattices with periodic boundary conditions and several lattice sizes$L$. The solid and the dotted line are fits to the Vogel-Fulcher and Adam-Gibbs equation, respectively. Data taken from Binder et al. [24].

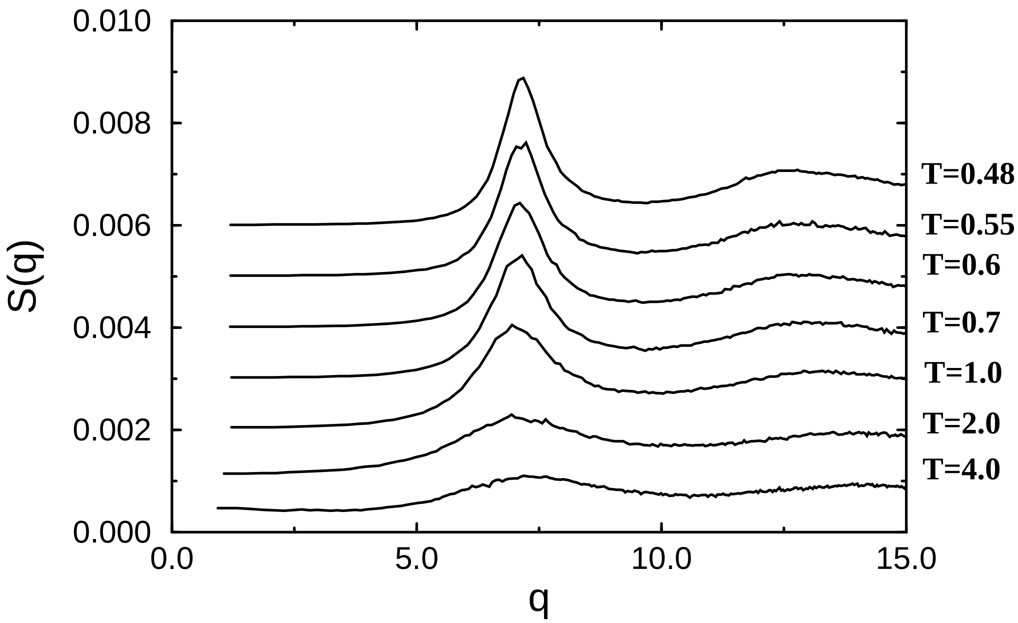

0.010
0.008
0.006
0.004
0.002
0.000
S(q)
0.0
5.0
10.0
15.0
q
T=0.48
T=0.55
T=0.6
T=0.7
T=1.0
T=2.0
T=4.0

FIG. 1.

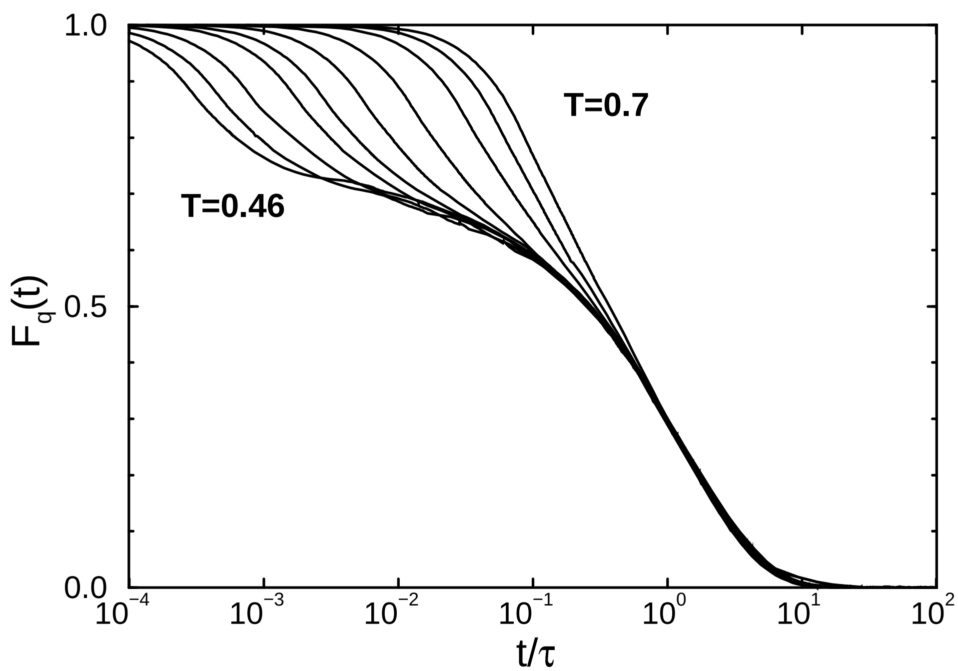

1.0
0.5
0.0
F_q(t)
T=0.7
T=0.46
10^-4
10^-3
10^-2
10^-1
10^0
10^1
10^2
t/τ

FIG. 2.

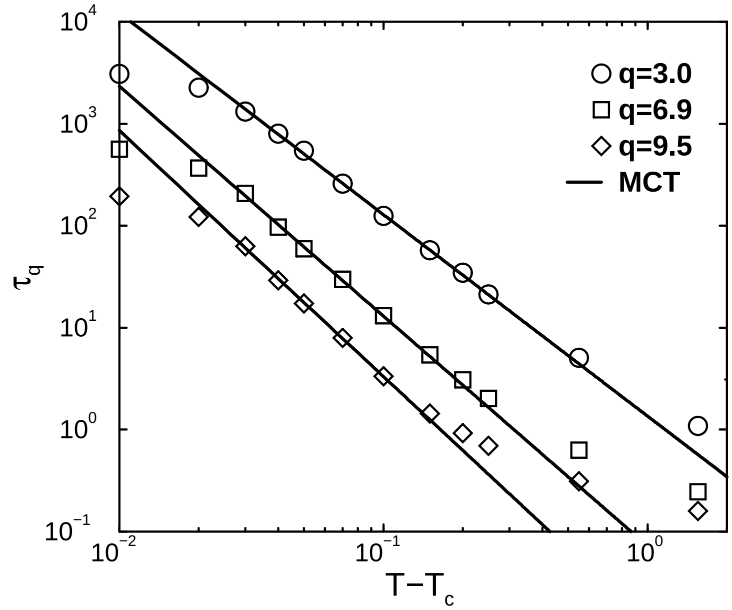

10^4
10^3
10^2
10^1
10^0
10^{-1}
τ_q
10^{-2}
10^{-1}
10^0
$T-T_c$
q=3.0
q=6.9
q=9.5
MCT

FIG. 3.

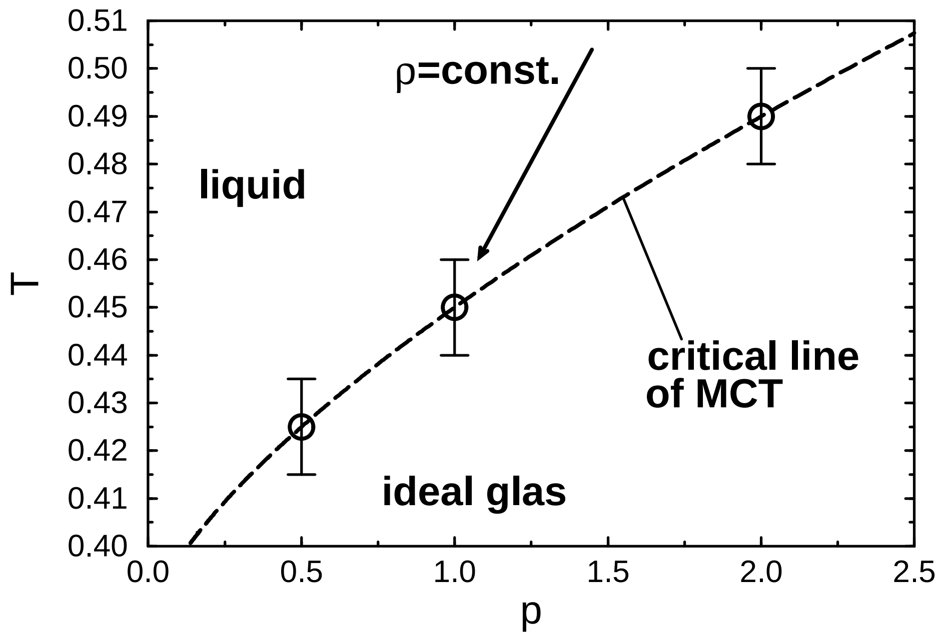

0.51
0.50
0.49
0.48
0.47
0.46
0.45
0.44
0.43
0.42
0.41
0.40
T
0.0
0.5
1.0
1.5
2.0
2.5
p
ρ=const.
liquid
critical line
of MCT
ideal glas

FIG. 4.

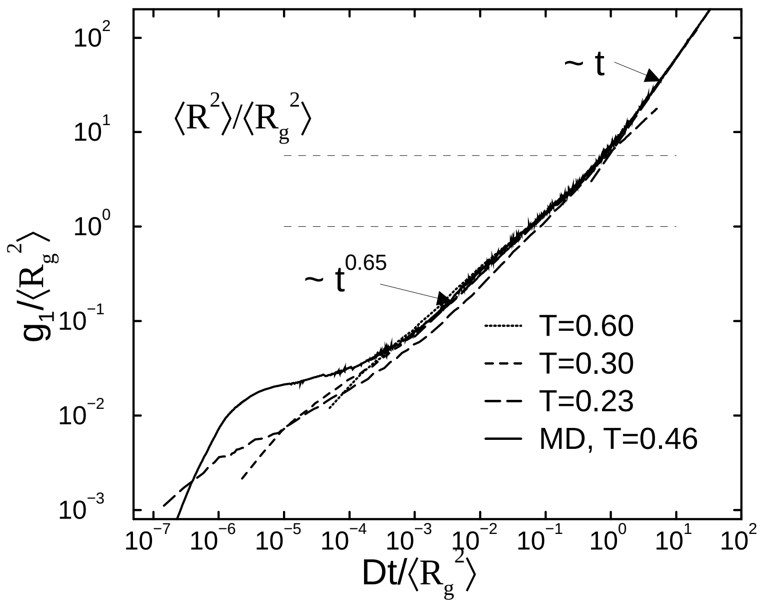

~ t
⟨R²⟩/⟨Rg²⟩
~ t^0.65
T=0.60
T=0.30
T=0.23
MD, T=0.46
g1/⟨Rg²⟩
Dt/⟨Rg²⟩

FIG. 5.

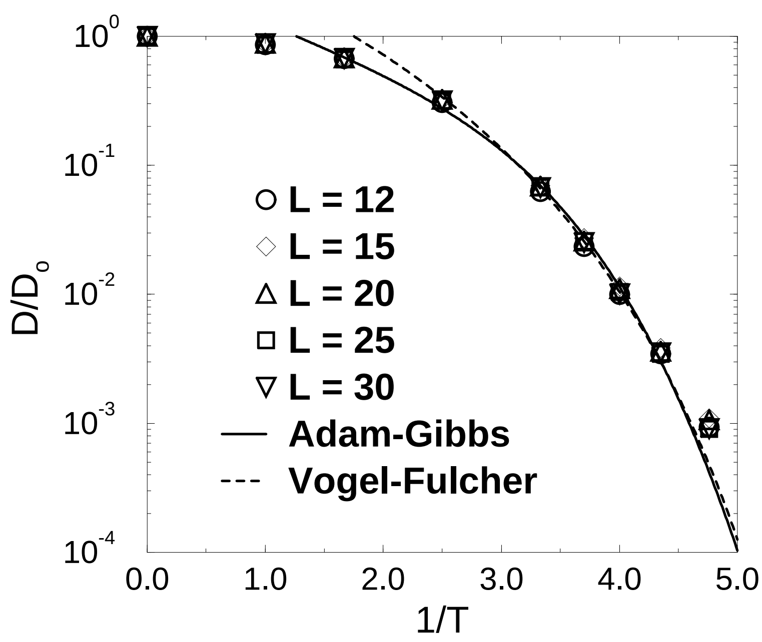

L = 12
L = 15
L = 20
L = 25
L = 30
Adam-Gibbs
Vogel-Fulcher
D/Do
1/T

FIG. 6.